Published in final edited form as:
J Struct Biol. 2009 October ; 168(1): 183–189. doi:10.1016/j.jsb.2009.02.008.

Supported double membranes

David H. Murray, **Lukas K. Tamm**, and **Volker Kiessling***
Center for Membrane Biology and Department of Molecular Physiology and Biological Physics, University of Virginia, 1340 Jefferson Park Avenue, Charlottesville, Virginia 22908

Abstract

Planar model membranes, like supported lipid bilayers and surface-tethered vesicles, have been proven to be useful tools for the investigation of complex biological functions in a significantly less complex membrane environment. In this study, we introduce a supported double membrane system that should be useful for studies that target biological processes in the proximity of two lipid bilayers such as the periplasm of bacteria and mitochondria or the small cleft between pre-and postsynaptic neuronal membranes. Large unilamellar vesicles (LUV) were tethered to a preformed supported bilayer by a biotin-streptavidin tether. We show from single particle tracking (SPT) experiments that these vesicle are mobile above the plane of the supported membrane. At higher concentrations, the tethered vesicles fuse to form a second continuous bilayer on top of the supported bilayer. The distance between the two bilayers was determined by fluorescence interference contrast (FLIC) microscopy to be between 16 and 24 nm. The lateral diffusion of labeled lipids in the second bilayer was very similar to that in supported membranes. SPT experiments with reconstituted syntaxin-1A show that the mobility of transmembrane proteins was not improved when compared with solid supported membranes.

Keywords

supported bilayer; tethered vesicles; fluorescence microscopy

INTRODUCTION

Biological membranes are characterized by their high level of complexity. Scaling down the complex real membranes to simpler model membrane systems has become a popular approach to achieve insights into the functions and interactions of their components. In recent years, supported bilayers (Tamm and McConnell, 1985) have received increasingly more attention due to their relative ease of preparation and their accessibility to sophisticated fluorescence techniques. Single particle techniques in particular are promising tools to gain detailed insight into biological mechanisms that are not accessible by ensemble measurements. Starting with the tracking of single lipids (Schmidt et al., 1995), supported membranes have since been employed in studies of more complex reactions such as e.g. single vesicle fusion (Bowen et al., 2004; Fix et al., 2004; Liu et al., 2005) and the fusion of single viral particles (Floyd et al., 2008). For a recent review on preparation and characterization methods of supported bilayers and their applications see (Kiessling et al., 2009).

*To whom correspondence should be addressed. Phone: (434)924-2752. Fax: (434)982-1616. vgk3c@virginia.edu.

In parallel to modeling membrane processes, an additional application of supported bilayers has emerged in recent years. Supported membranes can be utilized to anchor the tethers to vesicles that encapsulate molecules of interest (Boukobza et al., 2001) or that themselves act as the model membrane of choice (Yoshina-Ishii and Boxer, 2003). Like supported bilayers, surface- tethered vesicles have been used to gain insight into SNARE (soluble *N*-ethylmaleimide-sensitive-factor attachment protein receptor)-mediated neuronal vesicle fusion (Yoon et al., 2006). Tethering vesicles to a supported membrane has the advantage that nonspecific membrane surface interactions are reduced and, as a result, the observed reactions may more directly address the pertinent biological questions.

Our original motivation for this work was to develop a fusion assay with proteoliposomes that contain single copies of the fluorescently labeled transmembrane SNARE syntaxin-1A tethered to a supported bilayer. We utilized a biotin-streptavidin tether and found that most vesicles docked to supported bilayers that were prepared by a combined Langmuir-Blodgett / vesicle fusion (LB/VF) technique (Crane et al., 2005; Kalb et al., 1992) are laterally mobile above the supporting membrane. When vesicles were added at high concentrations, we found, to our surprise, that a second bilayer was formed on top of the first bilayer. These double membranes are comparable to systems that have been prepared by attaching much larger vesicles, giant unilamellar vesicles (GUV), to supported membranes as models for cell adhesion (Albersdorfer et al., 1997; Bruinsma et al., 2000; Kloboucek et al., 1999), or after rupturing as models for intermembrane junctions (Kaizuka and Groves, 2004; Wong and Groves, 2001). Since it is relatively easy to reconstitute membrane proteins into smaller proteoliposomes, we introduce our system as a new model to study biological processes distributed between or located in the proximity of two membranes such as the double membranes of Gram-negative bacteria or mitochondria, the synaptic cleft between neurons, or cell-cell adhesion contacts.

In the following, we first characterize the biotin-streptavidin tethered vesicles by single particle tracking (SPT) experiments. We then demonstrate the formation of a second bilayer by measuring the lateral diffusion of fluorescently labeled lipids by FRAP (fluorescence recovery after photobleaching) and the inter-membrane distance by FLIC (fluorescence interference contrast) microscopy. To test the feasibility of the double membranes as model systems we have reconstituted the transmembrane protein syntaxin-1A and characterized its mobility by SPT.

MATERIALS AND METHODS

The following materials were purchased and used without further purification: 1-palmitoyl-2-oleoyl-*sn*-glycero-3-phosphocholine (POPC), 1,2-dioleoyl-*sn*-glycero-3-phosphoethanolamine-N-[7-nitro-2-1,3-benzoxadiazol-4-yl] (NBD-DOPE), 1,2-dipalmitoyl-*sn*-glycero-3-phosphoethanolamine-N-[lissamine rhodamine B] (Rh-DPPE), 1,2-distearoyl-*sn*-glycero-3-phosphoethanolamine-N-[biotinyl (polyethylene glycol) 2000] (biotin-peg-DSPE), 1,2-dipalmitoyl-*sn*-glycero-3-phosphoethanolamine-N-[cap biotinyl) (biotin-cap-DPPE) (Avanti Polar Lipids, Alabaster, AL); Alexa Fluor 647 maleimide, Alexa Fluor 546 streptavidin and streptavidin (from *S. avidinii*) (Invitrogen, Carlsbad, CA); HEPES and glycerol (Sigma Chemical, St. Louis, MO); chloroform, ethanol, methanol, ether, Contrad detergent, all inorganic salts, acids, bases, and peroxide (Fisher Scientific, Fair Lawn, NJ).

Protein expression, purification and labeling

A more detailed description of the preparation of rat neuronal syntaxin-1A will be described elsewhere (Murray and Tamm, 2009). Briefly, syntaxin-1A lacking the regulatory H_{abc} domain (residues 183–288) was cloned into pET28b with the addition of a C-terminal cysteine to facilitate fluorescent labeling (Schuette et al., 2004). Following expression in BL21(DE3) cells, the N-terminal His-tagged protein was purified by affinity chromatography on Ni-NTA beads

(Fasshauer et al., 1998). After cleavage of the His-tag by thrombin, anion-exchange chromatography removed the His-tag and residual contaminants.

To fluorescently label syntaxin, DTT from the purification steps was first removed by dialyzing against 2 mM TCEP in purification buffer. The protein was then incubated with a 10-fold molar excess of Alexa647 maleimide overnight at 4 °C. Free dye was removed by size-exclusion chromatography followed by dialysis. Typically, labeling efficiencies of 40–55 % were achieved as determined by absorbance using manufacturer's extinction coefficients.

Large unilamellar vesicles

The desired lipids were codissolved in chloroform. Solvent was evaporated under a stream of N_2 gas followed by vacuum for at least 1 h. The resulting residue was suspended in reconstitution buffer (RB) consisting of 25 mM HEPES, 150 mM KCl, pH = 7.4, rapidly vortexed, freeze-thawed five times by submersion in liquid N_2 followed by water at 40 °C, and extruded by 15 passes through two polycarbonate membranes (Avestin, Ottawa, ON) with a pore diameter of 100 nm for the supported bilayer or 50 nm for the second bilayer. Vesicles were stored at 4 °C for up to 5 days before use.

Reconstitution of syntaxin in proteoliposomes

Beginning with dried lipid films, as prepared above, appropriate amounts of protein (1:25000 protein:lipid ratio) were added and incubated for 1–2 hours to solubilize the lipids and to form mixed protein/lipid/detergent micelles. Samples were diluted three-fold and dialyzed extensively against RB containing 1 mM DTT. Syntaxin was found to be oriented ~90 % right-side-out with the C-termini facing the lumen of the liposomes. This topology was determined by trypsin digestion and subsequent SDS/PAGE and by quenching of the Alexa fluorescence with cobalt. For single particle tracking experiments in double membranes, the sample was diluted by a factor of 100 with protein-free LUVs of the same lipid composition.

Planar supported bilayers

Supported bilayers were prepared by the LB/VF method (Kalb et al., 1992). On 40 mm × 25 mm × 1 mm quartz slides (Quartz Scientific, Fairport Harbor, OH) for FRAP and SPT or on 4-oxide FLIC chips (Braun and Fromherz, 1997) as described in detail earlier (Crane et al., 2005). Briefly, a POPC monolayer was spread from a chloroform solution onto a pure water surface in a Nima 611 Langmuir-Blodgett trough (Nima, Coventry, U.K.) and compressed to reach a surface pressure of 32 mN/m. A clean substrate was then rapidly dipped into the trough and slowly withdrawn, while a computer maintained a constant surface pressure and monitored the transfer of lipids onto the substrate by measuring the change in surface area. The slide or chip containing the resulting monolayer (LB monolayer) was then placed in a flow-through chamber (Tamm, 1993) and incubated with 1.2 ml of POPC vesicles containing 1 mol% biotin-peg-DPPE (90 μM total lipid) for 1–2 hours. Excess vesicles were washed out by extensive rinsing with RB.

Tethered vesicles and supported double membranes

After a supported bilayer had been prepared as described above, 1 ml of 2–4 μg/ml streptavidin was incubated with the bilayer for 15–30 minutes in the flow-through chamber and rinsed with 10 ml of RB. For tethered vesicle experiments, the membrane was then incubated with 1 ml of a low concentration of vesicles containing 0.1 mol% of biotin-cap-DPPE (4.5 μM total lipid). After 5–10 minutes, excess vesicles were washed out by rinsing with 10 ml RB. For double-bilayer experiments, 1 ml of 0.1 mol% biotin-cap-DPPE (0.1 mM total lipid) were incubated with the streptavidin-treated supported bilayer for 3–4 hours followed by rinsing with 10 ml RB.

Fluorescence microscopy

FRAP and FLIC experiments were performed on a Zeiss Axiovert 35 fluorescence microscope (Carl Zeiss, Thornwood, NY) with either a mercury lamp or an argon ion laser (Innova 300C, Coherent, Palo Alto, CA) as a light source. A mirror cube at the back of the microscope was used to switch between epi-illumination by the laser or lamp. A 40× water-immersion objective (Zeiss; numerical aperture (N.A.) 0.75) was used in all cases. For FRAP experiments, NBD-DOPE was excited by the laser @488 nm and observed through a 535-nm band-pass filter (D535/40, Chroma). The intensity of the laser beam was computer-controlled through an acoustooptic modulator (AOM-40, IntraAction, Bellwood, IL) or was blocked entirely by a computer-controlled shutter. For FLIC experiments, bilayers labeled with Rh-DPPE were excited with the mercury lamp through a 546-nm band-pass filter (BP546/10, Schott Glaswerke, Mainz, Germany) and observed through a 610-nm band-pass filter (D610/60, Chroma, Brattleboro, VT).

Images were recorded by an electron multiplying charge-coupled device (CCD) cooled to −70 °C (iXon DU860E-CSO-BV, Andor, Belfast, UK). Image analysis and data acquisition were accomplished using a custom-made program written in LabVIEW (National Instruments, Austin, TX).

FLIC microscopy

FLIC microscopy (Lambacher and Fromherz, 1996; Lambacher and Fromherz, 2002) was used to measure the average distance of all fluorescent dyes from a reflective interface. The details of the method, the optical model and parameters, fabrication of the substrates as well as a discussion of the accuracy have been described previously (Braun and Fromherz, 1997; Crane et al., 2005). In order to determine the average distance between the proximal and distal bilayer in the supported double membranes, we modified the optical layer model. In this case, the model consisted of seven layers: silicon, with refractive index n_{si} = 4.904 (435 nm), 4.138 (535 nm), 4.093 (545 nm), and 3.916 (610 nm) and attenuation index κ_{si} = 0.143 (435 nm), 0.036 (535 nm), 0.032 (545 nm), and 0.020 (610 nm) (Jellison, 1982); silicon oxide of known thickness d_{ox} and refractive index n_{ox} = 1.4696 (435 nm), 1.4634 (535 nm), 1.4630 (545 nm), and 1.4605 (610 nm) (Landoldt, 1962); a thin water-filled cleft of thickness d_{cleft} = 2 nm (Crane et al., 2005; Kiessling and Tamm, 2003) and refractive index n_{H2O}=1.333; the supported membrane of thickness d_{mem} = 4 nm (POPC) and refractive index n_{mem} = 1.45 (Gingell, 1979); the inter-membrane space between the two bilayers of thickness d_{im}, for which we assume the refractive index of water n_{H2O}; the second membrane of thickness d_{mem} and refractive index n_{mem} and the bulk water between the membrane and the objective with refractive index n_{H2O}.

FRAP

Bilayers were bleached in a pattern of parallel stripes (Smith and McConnell, 1978). The pixel intensities of images acquired before and after the bleach pulse were averaged and fit to the model:

$$F(t)=F_{\infty}+(F_0 - F_{\infty})e^{(-\mathrm{Da}^2 t)}, \quad (1)$$

where F_0 and F_∞ are the initial and final fluorescence intensities after bleaching, respectively, $a = 2\pi / p$, p is the stripe period (12.7 μm), and D is the lateral diffusion coefficient. The mobile fraction *m.f.*, which reflects the % of observed fluorescence recovery within the time frame of a FRAP experiment (30 s), is given by

$$m.f. = \frac{F_\infty - F_0}{F_{\text{pre}} - F_0} \times 200, \tag{2}$$

where F_{pre} is the fluorescence intensity before photobleaching. At least ten regions on five independently prepared bilayers were measured to determine the reported average values.

SPT

Single particle experiments were carried out with a Zeiss Axiovert 200 fluorescence microscope (Carl Zeiss), equipped with a 63× water immersion objective (Zeiss, N.A.=0.95) using a diode laser (Cube640-40C, Coherent) @640 nm or an argon ion laser (Innova 90C-5, Coherent) @514 nm as excitation source. The focused laser beam was directed through a trapezoidal prism onto the quartz-buffer interface where the membranes were attached. The prism-quartz interface was lubricated with glycerol to allow easy translocation of the sample cell on the microscope stage and to optically couple the prism and the slide. The beam was totally internally reflected at an angle of 72° from the surface normal, resulting in an evanescent wave that decays exponentially with characteristic penetration depths of 128 nm and 103 nm at excitation wavelengths of 640 nm and 514 nm respectively. An elliptical area of approximately 150 × 75 μm^2 was illuminated and observed. To track single Alexa647-syntaxin proteins, the fluorescent light was filtered by a dichroic mirror (660dclp, Chroma) and a long-pass filter (HQ665lp, Chroma). To track single Rh-DPPE labeled vesicles, the fluorescent light was filtered by a dichroic mirror (565dclp, Chroma) and a band-pass filter (D605/55, Chroma). Images were acquired by an electron multiplying CCD (iXon DV887ECS-BV, Andor). The CCD was cooled to −70 °C. During each acquisition, 50–100 images of 256 × 256 pixels were continuously recorded with an exposure time of 50 ms. The laser intensity, the shutter, and the camera were controlled by a home-made program written in LabVIEW (National Instruments).

Analysis of SPT data

Single molecule recognition and trajectory reconstructions were performed as previously described (Kiessling et al., 2006). Briefly, a home-made image analysis program in LabVIEW was used to first cross-correlate the images with the expected point spread function for particles at the diffraction limit (Gelles et al., 1988). Fluorescent spots were then recognized by the application of a threshold to the cross-correlated image, followed by a determination of the center of mass for each spot. Filtering criteria, such as the distance of a spot from the edge of the field of view and distance between particles, were then applied to remove particles from further evaluation. After a fit of a two-dimensional Gaussian profile to the original image using the center of mass as a starting coordinate, successive images were compared to reconstruct the trajectories of individual particles. Trajectories with at least 9 time steps (10 data points) were used in the analysis.

Mean-square displacements for four time lags were calculated according to (Kusumi et al., 1993; Schmidt et al., 1995):

$$\left\langle r^2 \right\rangle (t_{\text{lag}}) = \frac{1}{\sum_{t_i - t_j = t_{\text{lag}}}} \sum_{t_i - t_j = t_{\text{lag}}} \left(\vec{r}(t_i) - \vec{r}(t_j) \right)^2, \tag{3}$$

where $\vec{r}(t_i)$ and $\vec{r}(t_j)$ represent the positions of the fluorescent particle at times t_i and $t_j = t_i + t_{lag}$. The lateral diffusion coefficient D for free Brownian diffusion in the plane of the membrane is given by:

$$\langle r^2 \rangle = 4Dt_{lag} \quad (4)$$

Diffusion coefficients were determined from linear fits to the mean-square displacements (MSD) for individual trajectories and from all trajectories using the standard deviation of each MSD for each time-lag as weighting factor (Saxton, 1997). Particles that showed a diffusion coefficient <0.005 $\mu m^2/s$ were regarded as immobile.

The cumulative distribution was analyzed by pooling the square displacements r_i^2 from all trajectories. To calculate the diffusion coefficients, we fitted two models to the data. For each, we utilized the procedure described by Schütz et al. (Schütz et al., 1997) to fit the cumulative distribution function (CDF) for one or two freely diffusing fractions:

$$P(r^2, t_{lag}) = 1 - \left[\alpha \cdot \exp\left(-\frac{r^2}{\langle r_1^2 \rangle} \right) + (1 - \alpha) \exp\left(-\frac{r^2}{\langle r_2^2 \rangle} \right) \right] \quad (5)$$

with

$$\langle r_1^2 \rangle = 4D_1 t_{lag} \text{ and } \langle r_2^2 \rangle = 4D_2 t_{lag} \quad (6)$$

and the size of the larger fraction α (α = 1 in the case of one fraction).

RESULTS

Supported membrane

In order to prepare a surface with well-defined surface properties, we prepared biotinylated supported bilayers by the Langmuir-Blodgett/vesicle-fusion technique. Large unilamellar POPC vesicles that contained 1 mol% of biotin-peg-DSPE were added to supported monolayers composed of only POPC. The quality of these membranes was controlled by FRAP experiments with 0.5 mol% NBD-DOPE that was included in the bilayers. The diffusion coefficient was ~1 $\mu m^2/s$ with a mobile fraction of >90% (data not shown). We previously showed that supported bilayers prepared by the LB/VF method are nearly 100% asymmetric in their lipid distribution between the two leaflets (Crane et al., 2005). In a next set of experiments, we examined the specificity and efficiency of streptavidin binding to the biotinylated supported bilayer. Binding of 1 μg/ml of Alexa546-labeled streptavidin to supported membranes, was observed by total internal reflection fluorescence microscopy. As expected for the high-affinity biotin-streptavidin reaction (Green, 1990), binding to the 1 mol% biotin surface was very efficient and saturated within 15 min. No binding of streptavidin was observed when the membrane lacked biotin lipids (data not shown).

Tethered vesicles

LUVs containing 0.1 mol% biotin-cap-DPPE were added at low concentration to the streptavidin-treated supported bilayer. The vesicles contained either 0.5 mol% of Rh-DPPE (data not shown) or 0.004 mol% of Alexa647-labeled syntaxin. In both cases binding of the vesicles to the membrane was observed through a TIRF microscope. After a desired surface density of vesicles was reached (2–5 minutes), undocked vesicles were washed out and docked vesicles were tracked by acquiring series of 50–100 TIRF images at a rate of 20 Hz. The geometry of the resulting structure is shown in Figure 1A and a representative image is shown

in Figure 1B. We first computed the mean square displacements and performed a linear fit of Equation 3 to each trajectory. About 31 % of the docked vesicles were immobile and excluded from further evaluation. The mobile fraction was further evaluated by means of the cumulative distribution function (CDF) for the smallest time lag of 50 ms (Schütz et al., 1997). As shown in Figure 2 and Table 1, the data was best fit to Equation 5 with two different mobile fractions. In 90 % of the analyzed steps, the vesicles moved slowly with a diffusion coefficient of 0.13 $\mu m^2/s$, while 10 % moved faster with a diffusion coefficient of 0.52 $\mu m^2/s$.

We also performed some experiments, in which the first bilayer was prepared by direct vesicle fusion to the quartz instead of the combined LB/VF technique. Streptavidin binding to these supported bilayers was less efficient and all tethered vesicles were immobile (data not shown).

Supported double membranes

The proximal membrane with PEG-linked streptavidin was prepared in the same way as for the tethered vesicle experiments. To form a second bilayer on top, 1 ml of a more highly concentrated (0.1 mM total lipid) vesicle dispersion was added. In some experiments, we monitored the binding of the vesicles to the surface by taking TIRF images and computing the mean pixel intensities. Vesicle binding saturated after approximately 3 hours (data not shown). After three to four hours of incubation, unbound vesicles were washed out. To determine if the vesicles had laterally connected to form a second bilayer on top of the streptavidin layer, we added 0.5 mol% of NBD-DOPE to the vesicles and performed FRAP experiments. Pattern FRAP as employed here measures lipid diffusion over long distances (> 100 μm) and, therefore, high mobile fractions prove continuity of the bilayer on this length scale. We found that 87% of the labeled lipids were laterally mobile with a diffusion coefficient of 0.88 $\mu m^2/s$ (Table 1). This result indicates that a second bilayer had formed on top of the first layer as shown in Figure 1C. A fluorescence micrograph of the resulting membrane is shown in Figure 1D. The measured diffusion coefficient is similar to the ones that are found in quartz supported-membranes (Kiessling et al., 2006).

When the primary bilayer was prepared by the direct vesicle fusion technique, a layer was obtained that in some areas was uniformly fluorescent, but distinguished itself from a connected extended second bilayer by being essentially immobile in FRAP experiments. This behavior is characteristic of a layer of densely packed unfused vesicles that are not optically resolved. Other areas of the micrograph exhibited a more granular structure, and again no fluorescence recovery was observed in FRAP experiments. Therefore, the direct vesicle fusion method of primary bilayer formation was not further pursued in this work.

We also performed single particle tracking experiments, in which the second bilayer contained 4×10^{-5} mol% Alexa647-labeled syntaxin-1A. Approximately 10 % of the proteins were mobile. The cumulative distribution function for the squared distances was best fitted with two mobile fractions: a faster fraction with a diffusion coefficient of 0.25 $\mu m^2/s$ and a slower fraction with a diffusion coefficient of 0.03 $\mu m^2/s$ (Figure 2 and Table 1).

In order to confirm that the observed fluorescence originates from a membrane on top of and not from within the original supported bilayer, distances between the labeled membranes and the substrate surfaces were measured by FLIC microscopy. We first prepared supported bilayers by fusing LUVs containing 0.1 mol% biotin-cap-DPPE and 0.5 mol% Rh-DPPE to freshly cleaned 4-oxide FLIC chips (Braun and Fromherz, 1997; Kiessling and Tamm, 2003). An example of data and the corresponding best fit FLIC curves are shown in Figures 3A and C. In different preparations, this resulted in thicknesses between 1.4 and 1.8 nm, confirming previous results for supported bilayers (Crane et al., 2005; Fromherz et al., 1999; Kiessling and Tamm, 2003). In order to determine the distance between the two bilayers, the same experiment was performed on double membranes, in which only the second membrane was

labeled with Rh-DPPE. Compared with the previous result, we find a shift of the FLIC curve to the left and therefore an increased distance of the fluorophore from the substrate surface. For the example shown in Figures 3B and C this resulted in a distance of 14.6 ± 2.0 nm. From 81 fits of different areas of the same sample, we computed a mean distance of 16.6 ± 3.0 nm. Repeating the experiments with five different samples resulted in mean distances between 16 and 24 nm with standard deviations of ~3 nm. The statistical errors of the individual experiments as well as the variability between repeated bilayer preparations were significantly larger than the ones we obtained from single supported membrane experiments, where they were typically ±0.5 nm.

DISCUSSION

We have shown that single vesicles can be tethered efficiently to biotinylated supported membranes that have been treated with streptavidin. By reconstituting the transmembrane protein syntaxin-1A at single molecule concentrations into biotinylated vesicles, we utilized a concept introduced by Boukobza et al (Boukobza et al., 2001), who encapsulated single soluble proteins in a similar tethered vesicle system. However, in contrast to the earlier work, most of the tethered vesicles in our system are laterally mobile above the plane of the supported membrane proving minimal interactions between vesicles and the supported membrane surface. Our system is comparable in this regard to oligonucleotide-tethered vesicles on supported bilayers (Granéli et al., 2004; Yoshina-Ishii and Boxer, 2003). In our hands and in the particular system developed here, the method of forming the first supported bilayer is critical for the mobility of the tethered vesicles. Only bilayers that are prepared by the LB/VF technique (Crane et al., 2005; Kalb et al., 1992) result in mobile PEG-streptavidin-tethered vesicles.

When we incubated higher concentrations of vesicles for more than three hours, the preparation resulted in a second continuous bilayer on top of the first supported bilayer. The vesicles that we used to form the second bilayer were 50 nm in diameter and stayed intact when tethered to the first bilayer at low concentration. The formation of the second membrane is therefore consistent with two-phase models for the formation of supported membranes by the vesicle fusion technique (Johnson et al., 2002; Keller and Kasemo, 1998; Keller et al., 2000). Although we have not systematically investigated this issue, there appears to be no sharp transition from the tethered vesicle to the supported double membrane regime as a function of vesicle concentration because the process also appears to be kinetically controlled.

The diffusion of lipids over tens of microns is very similar to that observed in supported membranes, and the almost complete recovery of photobleached areas proves the integrity of a continuous second bilayer. The lipid diffusion rates in both membranes described herein are slower (~1 $\mu m^2/s$) compared to those observed in GUVs (3–5 $\mu m^2/s$, (Schwille et al., 1999)). This may mean that possible influences of the glass support on the diffusion in the supported membrane is transmitted also into the second membrane. We used FLIC microscopy to measure the distance between the two bilayers. The inter-membrane distances from different preparations varied between 16 and 24 nm. The fitting errors were larger than those resulting from measurements on standard supported membranes, but comparable to those obtained from experiments with GFP-tagged VAMP (vesicle associated membrane protein), which was located at a similar distance from the surface (Kiessling and Tamm, 2003). One reason for the increased fitting error is the heights of the oxide terraces. The distance of the second bilayer from the surface shifts the FLIC curve into a regime where the data points are close to extreme values (Fig. 3C). More accurate fits should be obtained by adapting the oxide heights to a more sensitive part of the FLIC curve. The lower end of the observed distance range is in good agreement with values that might be expected from the size of the cap-biotin-streptavidin-biotin-peg complex. The crystal structure of streptavidin reveals an approximately brick-

shaped molecule with 9.6 nm × 10.6 nm × 4.7 nm dimensions (Weber et al., 1992). The Flory radius of a randomly coiled PEG_{2000} molecule can be calculated to be 3.4 nm (de Gennes, 1987; Kunding and Stamou, 2006), while the total length of the extended polymer is 15.7 nm. Depending on the position of the streptavidin and assuming a randomly coiled polymer and a distance of ~1 nm between the biotin group and the secondary membrane surface, we expect an inter-membrane separation of at least 14 nm, i.e. slightly below the smallest measured values. The larger experimental distances could be due to bilayer undulations and partial extensions of the polymer. We also cannot exclude a systematic error due to incomplete bilayer formation of the top bilayer. A small fraction of unfused vesicles still adhering to the membrane could increase the observed FLIC distance without significantly influencing the observed mobile fraction in the FRAP experiments. However, this caveat does not impair the main conclusion of this work, namely that a second continuous bilayer has formed on top of the first bilayer.

The inter-membrane distances that we measured in our double membrane system are in between those reported for the two types of inter-membrane junctions between ruptured giant vesicles and supported bilayers (Kaizuka and Groves, 2004). In that work, Type 1 junctions are defined by a small separation distance of ~2.4 nm, while Type 2 junctions are characterized by a mean distance of ~50 nm and topographical undulations with a RMS amplitude of ~4 nm. The inter-membrane distance of the Type 1 junction of that work is similar to distances between fluid floating bilayers that are obtained by transferring four monolayers by the Langmuir-Blodgett and Langmuir-Schäfer techniques (Charitat et al., 1999; Fragneto et al., 2001). These latter distances were determined by neutron reflectometry to be between 2 and 3 nm.

The lateral diffusion of transmembrane proteins in the secondary bilayer was not improved when compared with proteins that were incorporated into standard supported bilayers made by the vesicle fusion technique. This result is most likely a consequence of the syntaxin orientation within the proteoliposomes. Since ~90 % of syntaxin molecules are facing with their N-terminal domains to the outside of the proteoliposomes, the 12 nm long SNARE domains (Sutton et al., 1998) of most proteins may be confined between the streptavidin molecules. This situation is different than in polymer-supported membranes where proteoliposomes of the same kind are fused with a lipid monolayer. After completion, most proteins in the latter system were mobile and oriented with their N-terminal SNARE motifs facing away from the surface (Kiessling and Tamm, 2003; Wagner and Tamm, 2001). Future combinations of the two systems and preparation techniques may allow us to prepare double membranes, in which membrane proteins in different bilayers have defined orientations, e.g. facing each other in the inter-membrane space or being directed outwards in specified orientations. The planar geometry and the availability of sophisticated detection and imaging techniques makes double membranes ideal models for mimicking small intracellular compartments, periplasms of bacteria or mitochondria, as well as cell adhesion contacts, for example those that form at neuronal synapses.

Acknowledgments

This work was supported by grants from the NIH.

REFERENCES

Albersdorfer A, Feder T, Sackmann E. Adhesion-induced domain formation by interplay of long-range repulsion and short-range attraction force: a model membrane study. Biophys. J 1997;73:245–257. [PubMed: 9199789]

Boukobza E, Sonnenfeld A, Haran G. Immobilization in surface-tethered lipid vesicles as a new tool for single biomolecule spectroscopy. J. Phys. Chem. B 2001;105:12165–12170.

Bowen ME, Weninger K, Brunger AT, Chu S. Single Molecule Observation of Liposome-Bilayer Fusion Thermally Induced by Soluble N-Ethyl Maleimide Sensitive-Factor Attachment Protein Receptors (SNAREs). Biophys. J 2004;87:3569–3584. [PubMed: 15347585]

Braun D, Fromherz P. Fluorescence interference-contrast microscopy of cell adhesion on oxidized silicon. Appl. Phys. A 1997;65:341–348.

Bruinsma R, Behrisch A, Sackmann E. Adhesive switching of membranes: Experiment and theory. Phys. Rev. E 2000;61:4253–4267.

Charitat T, Bellet-Amalric E, Fragneto G, Graner F. Adsorbed and free lipid bilayers at the solid-liquid interface. Eur. Phys. J. B 1999;8:583–593.

Crane JM, Kiessling V, Tamm LK. Measuring lipid asymmetry in planar supported bilayers by fluorescence interference contrast microscopy. Langmuir 2005;21:1377–1388. [PubMed: 15697284]

de Gennes PG. Polymers at an interface: a simplified view. Adv. Colloid Interface Sci 1987;27:189–209.

Fasshauer D, Eliason WK, Brunger AT, Jahn R. Identification of a minimal core of the synaptic SNARE complex sufficient for reversible assembly and disassembly. Biochemistry 1998;37:10354–10362. [PubMed: 9671503]

Fix M, Melia TJ, Jaiswal JK, Rappoport JZ, You D, Sollner TH, Rothman JE, Simon SM. Imaging single membrane fusion events mediated by SNARE proteins. PNAS 2004:7311–7316. [PubMed: 15123811]

Floyd DL, Ragains JR, Skehel JJ, Harrison SC, van Oijen AM. Single-particle kinetics of influenza virus membrane fusion. PNAS 2008;105:15382–15387. [PubMed: 18829437]

Fragneto G, Charitat T, Graner F, Mecke K, Perino-Gallice L, Bellet-Amalric E. A fluid floating bilayer. Europhys. Lett 2001;53:100–106.

Fromherz P, Kiessling V, Kottig K, Zeck G. Membrane transistor with giant lipid vesicle touching a silicon chip. Appl. Phys. A 1999;69:571–576.

Gelles J, Schnapp BJ, Sheetz MP. Tracking kinesin-driven movements with nanometer-scale precision. Nature 1988;331:450–453. [PubMed: 3123999]

Gingell DT, I. Interference reflection microscopy. A quantitative theory for image interpretation and its application tocell-substratum separation measurement. Biophys J 1979;26:507–526. [PubMed: 262429]

Granéli A, Edvardsson M, Höök F. DNA-Based Formation of a Supported, Three-Dimensional Lipid Vesicle Matrix Probed by QCM-D and SPR13. Chemphyschem 2004;5:729–733. [PubMed: 15179728]

Green, M. Methods in enzymology. Vol. Vol. Volume 184. Academic Press; 1990. Avidin and streptavidin; p. 51-67.

Jellison GEM, F.A. Optical constants for silicon at 300 and 10 K determined from 1.64 to 4.73 eV by ellipsometry. J. Appl. Phys 1982;53:3745–3753.

Johnson JM, Ha T, Chu S, Boxer SG. Early steps of supported bilayer formation probed by single vesicle fluorescence assays. Biophys. J 2002;83:3371–3379. [PubMed: 12496104]

Kaizuka Y, Groves JT. Structure and Dynamics of Supported Intermembrane Junctions. Biophys. J 2004;86:905–912. [PubMed: 14747326]

Kalb E, Frey S, Tamm LK. Formation of Supported Planar Bilayers by Fusion of Vesicles to Supported Phospholipid Monolayers. Biochim. et Biophys. Acta 1992;1103:307–316.

Keller CA, Kasemo B. Surface Specific Kinetics of Lipid Vesicle Adsorption Measured with a Quartz Crystal Microbalance. Biophys. J 1998;75:1397–1402. [PubMed: 9726940]

Keller CA, Glasmästar K, Zhdanov VP, Kasemo B. Formation of Supported Membranes from Vesicles. Phys. Rev. Lett 2000;84:5443–5446. [PubMed: 10990964]

Kiessling V, Tamm LK. Measuring distances in supported bilayers by fluorescence interference-contrast microscopy: polymer supports and SNARE proteins. Biophys J 2003;84:408–418. [PubMed: 12524294]

Kiessling V, Crane JM, Tamm LK. Transbilayer effects of raft-like lipid domains in asymmetric planar bilayers measured by single molecule tracking. Biophys J 2006;91:3313–3326. [PubMed: 16905614]

Kiessling, V.; Domanska, MK.; Murray, D.; Wan, C.; Tamm, LK. Wiley Encyclopedia of Chemical Biology. Vol. Vol. 4. John Wiley & Sons, Hoboken; 2009. Supported Lipid Bilayers: Development and Applications in Chemical Biology; p. 411-422.

Kloboucek A, Behrisch A, Faix J, Sackmann E. Adhesion-Induced Receptor Segregation and Adhesion Plaque Formation: A Model Membrane Study. Biophys. J 1999;77:2311–2328. [PubMed: 10512849]

Kunding A, Stamou D. Subnanometer actuation of a tethered lipid bilayer monitored with fluorescence resonance energy transfer. J Am Chem Soc 2006;128:11328–11329. [PubMed: 16939236]

Kusumi A, Sako Y, Yamamoto M. Confined lateral diffusion of membrane receptors as studied by single particle tracking (nanovid microscopy). Effects of calcium-induced differentiation in cultured epithelial cells. Biophys. J 1993;65:2021–2040. [PubMed: 8298032]

Lambacher A, Fromherz P. Fluorescence interference-contrast microscopy on oxidized silicon using a monomolecular dye layer. Appl. Phys. A 1996;63:207–216.

Lambacher A, Fromherz P. Luminescence of dye molecules on oxidized silicon and fluorescence interference contrast microscopy of biomembranes. J. Opt. Soc. Am. B 2002;19:1435–1453.

Landoldt, HB.; R. Numerical Data and Functional Relationships in Science and Technology. Vol. 6th ed.. Springer: Berlin: 1962.

Liu T, Tucker WC, Bhalla A, Chapman ER, Weisshaar JC. SNARE-Driven, 25-Millisecond Vesicle Fusion In Vitro. Biophys. J 2005;89:2458–2472. [PubMed: 16055544]

Murray DH, Tamm LK. 2009submitted

Saxton MJ. Single-Particle Tracking: The distribution of diffusion coefficients. Biophys. J 1997;72:1744–1753. [PubMed: 9083678]

Schmidt T, Schütz GJ, Baumgartner W, Gruber HJ, Schindler H. Characterization of Photophysics and Mobility of Single Molecules in a Fluid Lipid-Membrane. J. Phys. Chem 1995;99:17662–17668.

Schuette CG, Hatsuzawa K, Margittai M, Stein A, Riedel D, Küster P, König M, Seidel C, Jahn R. Determinants of liposome fusion mediated bz synaptic SNARE proteins. PNAS 2004;101:2858–2863. [PubMed: 14981239]

Schütz GJ, Schindler H, Schmidt T. Single-molecule microscopy on model membranes reveals anomalous diffusion. Biophys. J 1997;73:1073–1080. [PubMed: 9251823]

Schwille P, Korlach J, Webb WW. Fluorescence correlation spectroscopy with single-molecule sensitivity on cell and model membranes. Cytometry 1999;36:176–182. [PubMed: 10404965]

Smith BA, McConnell HM. Determination of molecular motion in membranes using periodic pattern photobleaching. PNAS 1978;75:2759–2763. [PubMed: 275845]

Sutton RB, Fasshauer D, Jahn R, Brunger AT. Chrystal structure of a SNARE complex involved in synaptic exocytosis at 2.4 Angstroem resolution. Nature 1998;395:347–353. [PubMed: 9759724]

Tamm, LK. Optical Microscopy: Emerging Methods and Applications. San Diego, CA: Academic Press; 1993. Total internal reflectance fluorescence microscopy; p. 295-337.

Tamm LK, McConnell HM. Supported Phospholipid-Bilayers. Biophys. J 1985;47:105–113. [PubMed: 3978184]

Wagner ML, Tamm LK. Reconstituted syntaxin1A/SNAP25 interacts with negatively charged lipids as measured by lateral diffusion in planar supported bilayers. Biophys. J 2001;81:266–275. [PubMed: 11423412]

Weber PC, Wendoloski JJ, Pantoliano MW, Salemme FR. Crystallographic and thermodynamic comparison of natural and synthetic ligands bound to streptavidin. J. Am. Chem. Soc 1992;114:3197–3200.

Wong AP, Groves JT. Topographical Imaging of an Intermembrane Junction by Combined Fluorescence Interference and Energy Transfer Microscopies. J. Am. Chem. Soc 2001;123:12414–12415. [PubMed: 11734045]

Yoon T-Y, Okumus B, Zhang F, Shin Y-K, Ha T. Multiple intermediates in SNARE-induced membrane fusion. PNAS 2006;103:19731–19736. [PubMed: 17167056]

Yoshina-Ishii C, Boxer SG. Arrays of Mobile Tethered Vesicles on Supported Lipid Bilayers. J. Am. Chem. Soc 2003;125:3696–3697. [PubMed: 12656589]

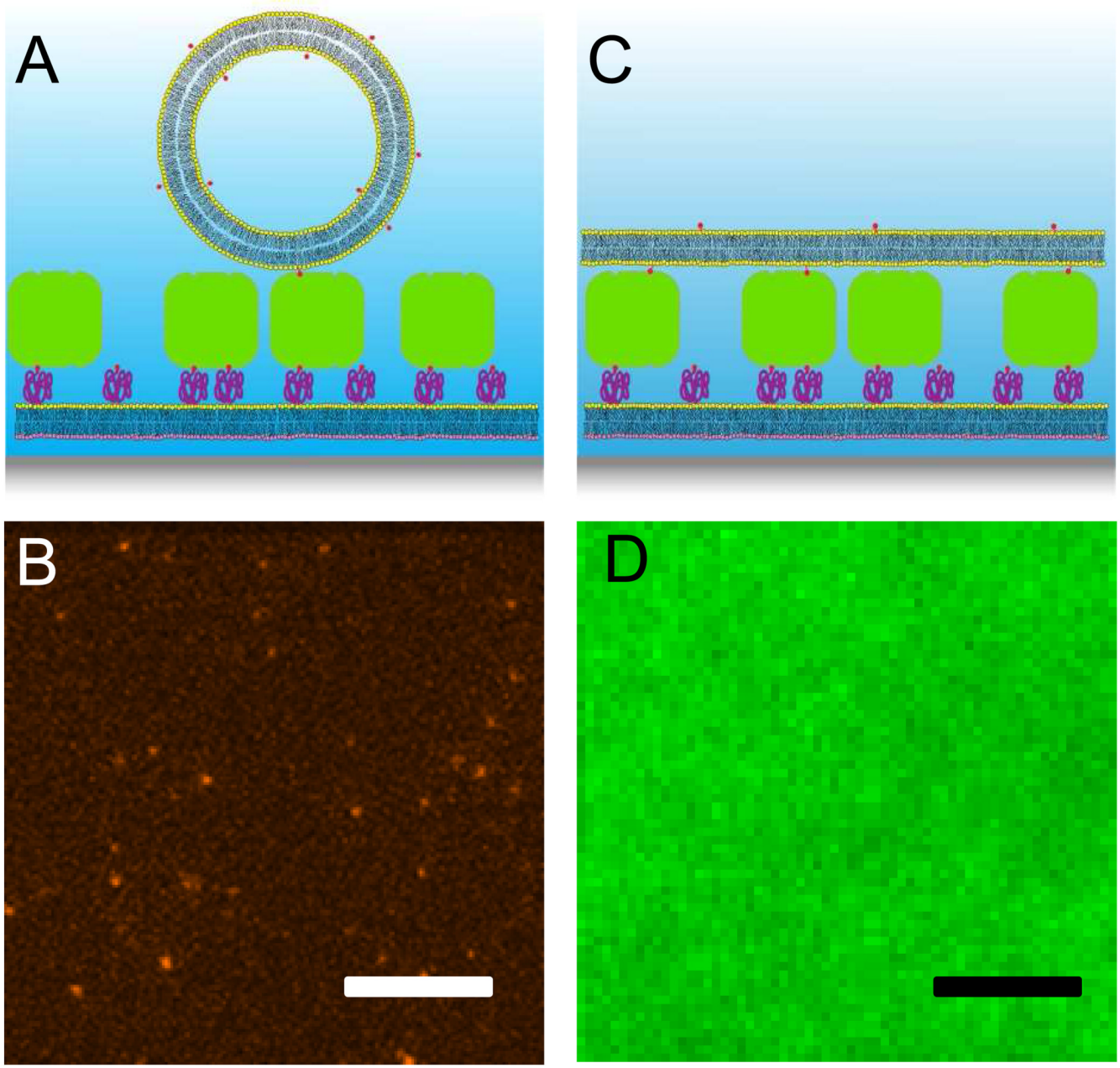

Figure 1.
Membrane-tethered vesicles and supported double membrane. A: Biotinylated vesicles tethered by streptavidin to a biotin-PEG-doped supported bilayer. System components are not drawn to scale. B: Fluorescence micrograph of tethered vesicles, doped with Alexa647-syntaxin-1A. Scale bar: 10 μm. C: Supported double membrane. Tethered vesicles formed a second bilayer on top of the first; the inter-membrane space is bridged by the PEG-biotin-streptavidin-biotin-cap tethers. D: Fluorescence micrograph of a NBD-DOPE-doped supported double membrane. Scale bar: 10 μm.

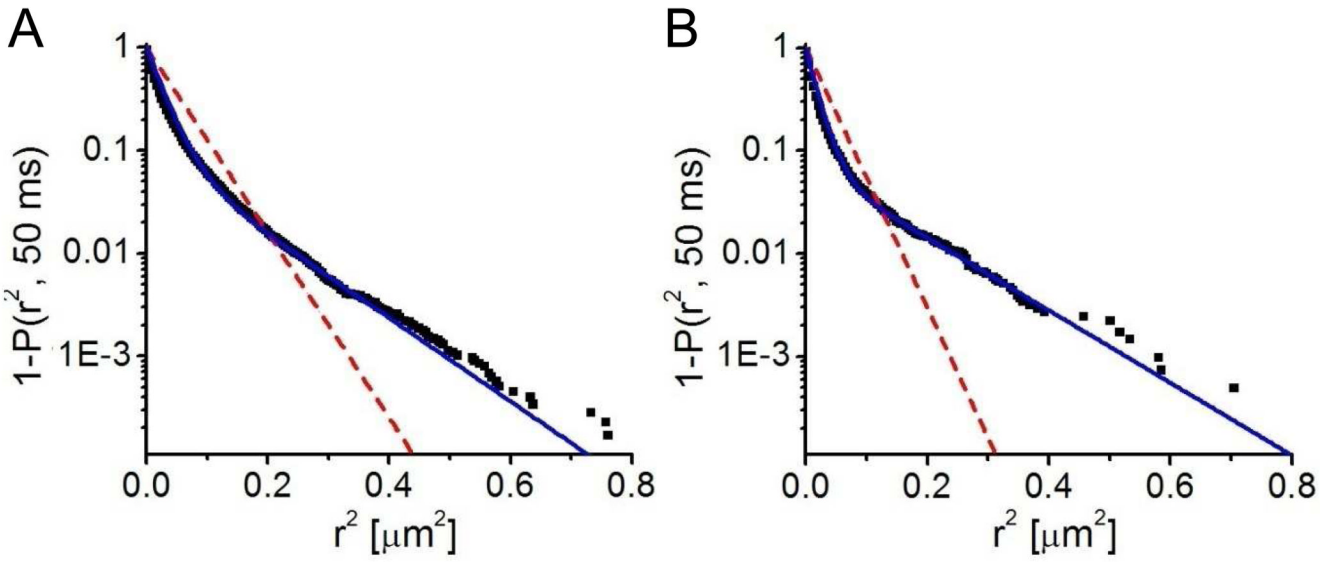

Figure 2.

Cumulative distribution functions derived from SPT data of tethered vesicles (A) and supported double membranes (B). Both systems contained single-molecule concentrations of Alexa647-labeled syntaxin-1A. From reconstructions of the particle trajectories, the cumulative distribution functions for the smallest time lag were generated. Fits to one-fraction diffusion are shown as red dashed lines, and fits to the two-fraction diffusion model are shown as solid blue lines. The best fit results and statistics are listed in Table 1.

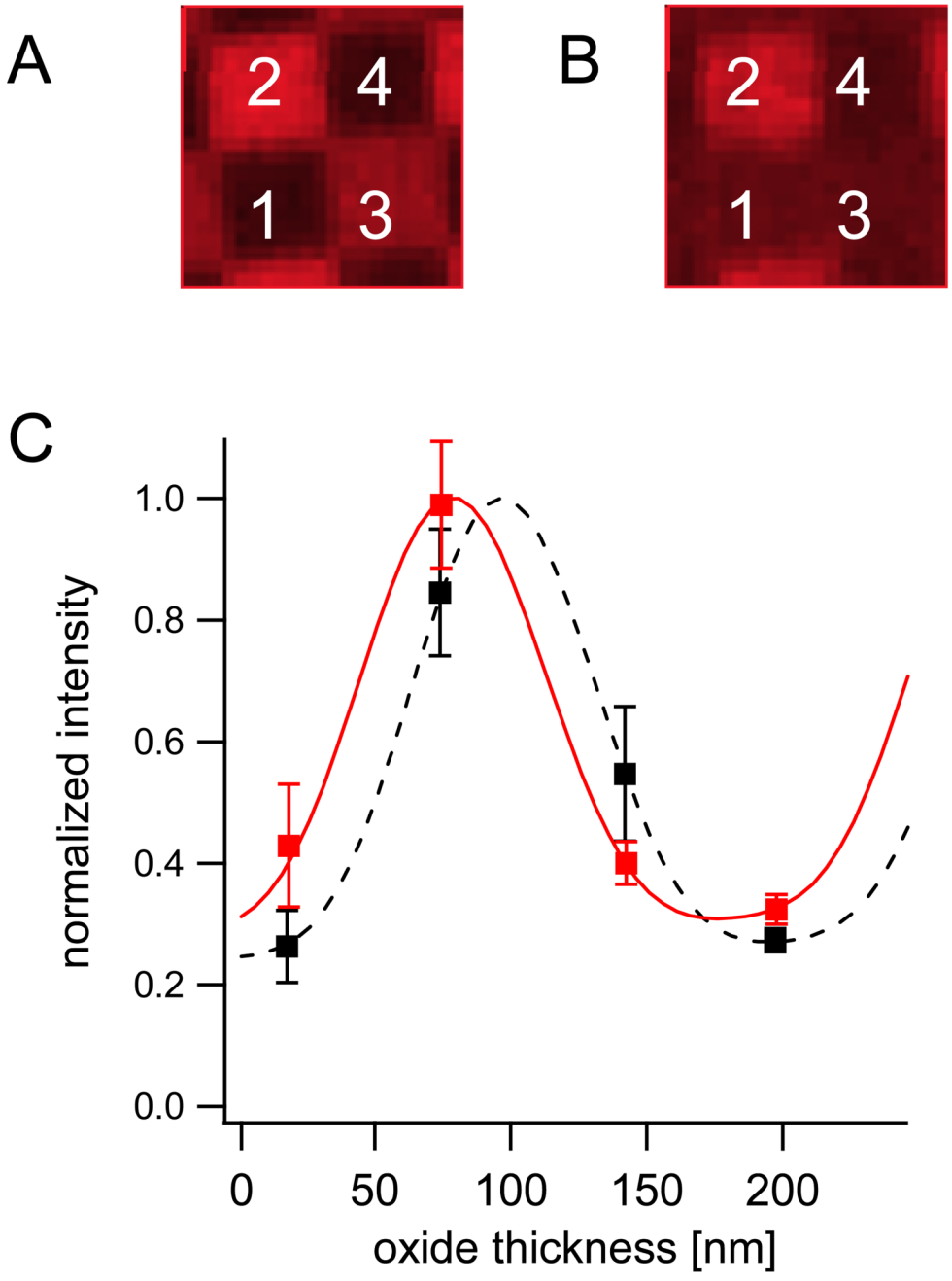

Figure 3.

FLIC measurements. A: Fluorescence micrograph of Rh-DPPE-doped supported bilayer on 4-oxide FLIC chip. Numbers indicate the 4 oxide levels. Width of one square is 5 μm. B: Fluorescence micrograph of Rh-DPPE-doped supported double membrane on 4-oxide FLIC chip. C: FLIC data and fitted theory of supported bilayer (dashed black) and supported double membrane (solid red). Mean intensities and standard deviations of the fluorescence intensities were extracted from the four oxide levels in A and B. The supported bilayer data was fitted with a membrane-substrate distance of 1.7 ± 0.7 nm. The supported double membrane was fitted with an inter-membrane distance of 14.6 ± 2.0 nm.

Table 1

Diffusion characteristics of supported membrane-tethered vesicles and supported double membranes.

	FRAP (NBD-DOPE)			SPT (Alexa647-syntaxin)				
	D ($\mu m^2/s$)	m.f.[a] (%)	n[c]	D_1 ($\mu m^2/s$)	D_2 ($\mu m^2/s$)	α[b]	m.f.[a] (%)	n[c]
Tethered Vesicles	-	-	-	0.13±0.03	0.52±0.01	0.90±0.01	69	7
Supported double membranes	0.88±0.02	87±1	5	0.032±0.004	0.246±0.002	0.86±0.01	10	16

[a] mobile fraction

[b] slow fraction

[c] number of samples